Chapter 7

Calcium Phosphate/Clay Nanotube Bone Cement with Enhanced Mechanical Properties and Sustained Drug Release

Udayabhanu Jammalamadaka, Karthik Tappa and David K. Mills

Additional information is available at the end of the chapter

http://dx.doi.org/10.5772/intechopen.74341

Abstract

Calcium phosphate cement (CPC) has limited use in bone repair due to their poor mechanical properties. Halloysite nanotubes (HNTs) are clay tubes with an aluminosilicate composition. The physicochemical properties, cytocompatibility, and cellular response to the CPC/HNT composites were assayed. Compression strength, FTIR analysis, protein synthesis, and mineralization were assessed. The cumulative data show that composites of tricalcium phosphate (TCP), anhydrous calcium diphosphate (DCPA) as the solid phase agent, and 10% chitosan lactate solution as the setting liquid produced cement with sustained release properties without loss of material strength. The composite also showed enhanced material properties (adhesiveness, surface roughness, and increased strength). Cellular assays confirm its osteoconductive and osteoinductive nature. CPCs, loaded with gentamicin- and neomycin-doped HNTs, showed sustained antibacterial release and marked zone of growth inhibition. CPCs fabricated with drug-doped HNTs offer a means for inducing bone growth at the site of implantation while controlling infection. This treatment modality should hasten patient healing time and enhance restoration of function. The increase in materials properties suggests that this CPC may be clinically applied to repair injuries in load-bearing bones.

Keywords: bone cement, bone repair, calcium phosphate, halloysite nanotubes, osteoblasts, sustained release, tissue engineering

1. Introduction

Polymethylmethacrylate (PMMA) is widely commercially used bone cement [1, 2]. The most common method of application is the dry mixing of drugs along with the bone cement and administering it into the body [3]. While long considering the 'gold' standard in local antibiotic therapy, it has many disadvantages. A radiolucent fibrous tissue is often observed at the bone/cement interface due to the release of toxic methylmethacrylate (MMA) monomers which damages surrounding tissue [3, 4]. These cements also exhibit a high exothermic setting temperature. Temperatures ranging from 70–120°C have been reported during setting of the PMMA bone cement during implantation [2, 5]. In an experiment conducted by Stańczyk and Rietbergen on bovine cancellous bone, the temperature exposure of 70°C by a fraction (10%) of the bone at the bone/cement interface was recorded [6]. The addition of antibiotics results in reduced mechanical properties in the cement [7]. Furthermore, the release of the antibiotic is short lived and results in less than maximal antibiotic release [7, 8]. Finally, PMMA cements lack elasticity and have dense structure which does not allow bone growth inside the cement [9].

Brown and Chow were the first to propose the use of calcium phosphate cement (CPC) in bone repair [10]. CPC was approved in 1996 by the Food and Drug Administration (FDA) for repairing craniofacial defects [11]. CPCs have many advantages over PMMA cement. Low shrinkage, durable, dense or porous (depending on the site of injury), and formability (ability to fill cavities of complex configurations) are additional positive qualities of CPCs [12–14]. Due to their similarity to apatite minerals in natural bone, calcium phosphate (CaP) bioceramics, such as hydroxyapatite (HA), are osteoconductive and osteoinductive [15–17]. CPCs implants provide an ideal environment for colonization by osteoblasts to form a functional interface [18, 19]. The end product is easily resorbed by osteoclast cells, leading to new natural bone formation at the bone-implant interface [21].

All CPCs are formulated by mixing a solid and a liquid component. The solid component consists of two or more calcium phosphate salts. The solid phase usually consists of a basic and an acidic salt, which reacts together in an aqueous medium and precipitates HA as a final product [19, 20]. The liquids used can be either water, alginates, chitosan, or sodium phosphates [20–22]. To obtain maximum biological use, these components are mixed in predetermined proportions that will lead to the formation of HA. Resorbability of the CPCs completely depends on its end product [22]. The physicochemical reactions that occur during mixing are complex, and cement setting time depends on factors such as solid-liquid composition, liquid-to-powder ratio, and particle size of the powder. Setting conditions also influence the mechanical properties of the cement [23]. However, due to its brittleness, CPCs are restricted to the reconstruction of non-loading bearing bone [24, 25]. Recently, absorbable fibers [23] and chitosan [26] were used to improve the load-bearing capability of CPC [27, 28]. Chitosan and its derivatives are natural biopolymers that are biocompatible, biodegradable, and osteoconductive [29]. CPCs can also be modified through additives (i.e., silicon, strontium, and zinc) and delivered as paste, putty or in an injectable form and set *in situ* to provide intimate adaptation to complex-shaped defects [23, 24]. Polymer materials added as an organic phase to the CPCs have been shown to improve the biological response, physicochemical, and mechanical properties, such as injectability, cohesion, resorption, and toughness [27, 28, 30].

Halloysite nanotubes (HNTs) are commercially inexpensive and two-layered aluminosilicate nanotubes are found naturally as raw mineral deposit. When dehydrated, 15–20 clay layers form a hollow tubule which is capable of carrying drugs [31, 32]. Inside of the lumen is positively charged and the external surface is negatively charged, permitting additional functional modifications of these surfaces. This charge on both outer and inner surfaces affects the efficiency of loading drugs and chemical agents [33, 34]. Substances with overall negative charge can be easily loaded into the lumen when compared to positively charged particles. The size of HNTs varies from 500 to 1000 nm with an inner diameter of 15–100 nm depending on the deposit [35]. Due to physical properties such as nanosized lumens, high L/D (length to diameter) ratio, low hydroxyl group density, low cost, and abundant natural deposits, HNTs have been intensely studied as a controlled or sustained release agent [31, 33, 34]. Loading HNTs with pharmaceuticals showed low initial release concentrations, preventing an initial outburst and uniform drug delivery (particularly with drugs, such as antibiotics, hormones, and growth factors) [35–37]. The drugs dexamethasone, furosemide, and nifedipine gave an extended 6–10 h release profile [29]. Under optimal conditions, a maximum loading of 12% volume (very close to theoretical capacity) was obtained [29]. When HNTs are added to polymeric materials, they improve material and mechanical performance and stability [34]. HNTs have been used to increase surface area, impart high surface reactivity, and improve mechanical strength with a relatively low cost [32, 34]. To achieve an increase in the toughness, mechanical strength, and thermal stability, HNTs have incorporated into a variety of polymers and examples include: poly(methyl-methacrylate) [35], poly(butylene succinate) [38], polyamide [12, 39], styrene-butadiene [40], epoxy [41], and chitosan [42]. In two previous studies using electrospinning, HNTs were used to enhance the polymer material properties including biological, chemical, mechanical, and thermal properties (see Kamble et al., (2012) for a more detailed review) [34].

Presently, the use of CPCs in regenerative medicine and orthopedic surgery is limited only to non-load bearing regions, that is, cranioplasty [43, 44]. There is a critical need for developing osteogenic and osteoconductive cement that can be used in load-bearing sites. The objective of this study is to improve the mechanical and anti-infective properties of CPCs. The common thread between these two objectives is the use of HNTs to provide a means for sustained release of anti-infective agents (gentamicin sulfate and neomycin sulfate) and to improve the material properties (tensile strength and adhesiveness) of the cement. The choice of CPC component materials was also a critical factor.

2. Materials and methods

2.1. Materials

Calcium phosphate dibasic anhydrous ($HCaO_4P$, DCPA), β-tri calcium phosphate ($Ca_3O_8P_2$, β-TCP), calcium phosphate monobasic monohydrate ($H_4\ CaO_8\ P_2\ H_20$, MCPM), chitosan oligosaccharide lactate ($(C_{12}H_{24}N_2O_9)_n$), chitosan (low molecular weight), dexamethasone, gentamicin, neomycin, calcium L-lactate ($C_6H_{10}CaO_6 \times H_2O$), and HNTs ($H_4Al_2O_9Si_2\ 2H_2O$) were purchased from Sigma-Aldrich, St. Louis, MO. Tetra calcium phosphate (Ca_4O_4P, TTCP) was ordered from CaP Biomaterials, E. Troy, WI. Cupric chloride ($CuCl_2$) and calcium carbonate ($CaCO_3$) were delivered

from Nasco, Fort Atkinson, WI. Sodium phosphate dibasic (Na_2HPO_4) was purchased from Fisher Scientific Company, Waltham, MA. Human osteoblast cells (C-12760) and osteoblast growth medium were purchased from PromoCell, Heidelberg, Germany. Mouse pre-osteoblast cell lines MC3T3-E1 (ATCC® CRL-2593™) and mouse bone marrow stromal cells (MSCs) CRL-12424 (ATCC® CRL-12424™) were obtained from ATCC (Manassas, VA.). Cell culture and lab plastics were obtained from MidScientific, St. Louis, Mo. Alpha minimal essential medium (α-MEM) and Dulbecco's DMEM were obtained from GIBCO Invitrogen, Grand Island, NY. Fetal bovine serum and penicillin-streptomycin were purchased from Phenix Research Products (Candler, NC). TryplE, an animal free trypsin substitute, and Trypan blue were obtained from GIBCO Invitrogen, (Grand Island, NY). Cell Titer Blue assay was purchased from Promega (Sunnyvale, CA). The Picrosirius red staining kit was obtained from Polysciences, Inc. (Warrington, PA.)

2.2. Sample preparation

Different types of calcium phosphate salts were mixed in different proportions using various chemicals as part of the liquid phase to identify the best composition with respect to their mechanical properties (**Table 1**). All samples were mixed using mortar and pestle under ambient conditions (room temperature and atmospheric pressure). The powder phase was mixed thoroughly until all the salts were uniformly dispersed. To this, the liquid phase was added in small quantities and triturated until the mixture became a thick, moldable paste.

The most suitable formulation was achieved when tetracalcium phosphate (TTCP provided by CaP Biomaterials) and dicalcium phosphate (DCPA provided by Sigma-Aldrich, St. Louis, MO.) were used as the solid phase and chitosan lactate (CL) was used as the setting liquid. An equimolar ratio of TTCP and DCPA was mixed and to this 10% w/v solution of CL was added. This mixture was thoroughly mixed using mortar and pestle to form a soft mass. The soft mass could then be set in different mold shapes depending on the assay or test being performed.

2.2.1. Sample preparation for SEM

Scanning electron microscopy (SEM) was used to analyze the surface of CPCs. Specimens fractured during compression test were taken for SEM imaging. S4800 Field Emission SEM, HITACHI was used for our research. Gold nanolayer (about 3 nm) was laid over specimens before analyzing using SEM.

Group	CPC Composition
Group 1	CPC powder without HNTs
Group 2	CPC powder with 5% wt. HNTs
Group 3	CPC powder with 10% wt. HNTs
Group 4	CPC powder with 15% wt. HNTs

Table 1. Control and experimental groups use in osteoconductive studies.

2.2.2. Compression strength testing

Compression test was performed on cylindrical shape specimens (12 mm length and 6 mm diameter). Compression test was performed on dry specimens and on specimens placed in simulated biological fluid (SBF) for 24 h before testing. Testing was done using an ADMET tensile tester with a load speed of 1 mm/min. FTIR spectroscopy was done to analyze the composition of CPCs after setting.

2.2.3. Flexural strength testing

Samples of dimensions 65 mm × 10 mm × 4 mm were prepared using paraffin wax in accordance with the ASTM F417-78 standards. Cement samples were put in these molds and used for flexural testing. The same compression machine was used at a cross-head speed of 1 mm/min. Three samples for each concentration of HNTs were used and an average was calculated.

2.3. FTIR analysis

Potassium bromide (KBr) pellet method was used for FTIR spectroscopy. Thin discs of KBr were prepared by placing a small amount of KBr into the die set and were subjected to a pressure of 8 tons. This pressure caused the KBr to re-crystallize to form thin transparent discs. These discs were used to obtain the background. A small amount of test sample powder was added to KBr and thin discs were prepared by a similar procedure.

2.4. Loading of the HNTs with dexamethasone (DEX)

HNTs were loaded using the vacuum loading technique. Saturated solution of Dex was made by dissolving 200 mg of Dex in 50 mL of ethanolic water (50%v/v). To this solution, 9 g of HNTs were added and subjected to vacuum cycles. The suspension of HNTs in Dex was kept in a vacuum for 20 min and at atmospheric pressure for 20 min, this was repeated thrice. This suspension was left under the vacuum overnight and centrifuged. The supernatant was discarded and HNTs were washed twice with deionized water to remove drug adsorbed on the HNT surface. Washed HNTs were dried in a vacuum and these were used in further experiments.

Drug release from HNTs was measured for a period of 96 h. Accurately measured quantity of 50 mg of Dex loaded HNTs was taken in a centrifuge tube and 1 mL of simulated biological fluid (SBF) was added and placed in a shaker. After specific time intervals, the tube was centrifuged to precipitate HNTs and the supernatant was collected. Equal volume of SBF was replaced every time supernatant was collected to maintain sink conditions. Collected supernatant was observed using a UV-visible spectrophotometer (NanoDrop) at a wavelength of 240 nm.

2.5. Cell culture, proliferation, and differentiation

Mouse pre-osteoblast cell lines MC3T3-E1 (ATCC® CRL-2593™) were obtained from ATCC (Manassas, VA.). Mouse pre-osteoblast (OB) was used for evaluating the osteoconductive potential CPC/HNT composites (details are provided below). OBs were maintained in a minimum essential medium, Eagle's α-modification (α-MEM), containing ribonucleosides,

deoxyribonucleosides, sodium bicarbonate, and supplemented with 2 mM L-glutamine, 1% antibiotics (100 U/mL penicillin and 100 U/mL streptomycin), and 10% fetal bovine serum (FBS) (complete α-MEM). Cells from passage 3 to 4 were used.

Mouse bone marrow stromal cells (MSCs) CRL-12424 (ATCC® CRL-12424™) were used for evaluating the osteoinductive potential CPC/HNT composites (details are provided below). MSCs were maintained in Dulbecco's Modified Eagles Medium (DMEM) with 10% FBS and 1% antibiotics (100 U/mL penicillin and 100 U/mL streptomycin (complete DMEM)). Cells from passage 3 to 4 were used.

Human osteoblast (HOB) cells were used to assess potential cytotoxicity issues. HOBs were cultured in osteoblast growth media according to the manufacturer's directions. Cells from passage 2 to 3 were used.

2.5.1. Cell proliferation

To check the cytocompatibility of the formulated scaffolds, XTT was performed on human osteoblast (HOB) cells C-12760 purchased from PromoCell, Heidelberg, Germany. XTT assay kit (X4751) with 1% PMS was ordered from Sigma-Aldrich. CPC discs of 5 mm × 1 mm dimensions were molded using different concentrations of HNTs (5, 10, and 15%). Control discs without any HNTs and blank cell lines were also cultured for comparative studies.

XTT or 2,3-bis-(2-methoxy-4-nitro-5-sulfophenyl)-2*H*-tetrazolium-5-carboxanilide is a sensitive and reliable quantitative assay. It is a colorless or slightly yellow color tetrazolium dye which gets converted into bright orange color formazan on reduction. When this dye is used in cell cultures, the dehydrogenase enzymes produced from mitochondrial cycle of actively respiring cells reduces the dye to orange color formazan. This assay is greatly improved by adding an electron accepting agent such as PMS (*N*-methyl dibenzopyrazine methyl sulfate). Unlike MTT, this assay does not require to go through laborious procedures such as solubilization prior to quantization, making this process quick and easy. Osteoblast cells, upon reaching to 90% confluency, were trypsinized and resuspended into culture media. In a 96 well plate, 100 μL of cell suspension was added in each well and incubated for 24 h. Activated XTT solution (20 μL) was then added to each well and incubated for 2 h and optical densities were measured using a Phenix LT-4000 absorbance microplate reader at 450 nm.

2.5.2. Assessment of CPC/HNT osteoconductive and osteoinductive potential

For seeding into CPC/DEX (+/−)/HNTs, OBs and MSCs were detached from the flasks by adding TryplE, an animal free trypsin substitute, and mixed with HBSS. Cells were then centrifuged and the cell pellets resuspended in either complete α-MEM or DEM. Setting liquid remained the same for all the formulations except for changes in solid components as described below.

For cell-culture techniques, disc-shaped specimens 10 × 2 mm were made using steel molds. The liquid phase used in this process was prepared from sterile deionized water. After setting, the samples were removed from the molds, dipped in alcohol, and dried under a class II hood.

Two different scaffold types were made for culturing cells (**Tables 1** and **2**). One set of scaffolds were made to evaluate the osteoconductive nature of CPCs while the other set was used to assess its osteoinductive potential. Osteoconductive scaffolds contained CPC powder with varied amounts of HNTs (**Table 1**). Four groups were prepared containing 0, 5, 10, and 15% wt. of HNTs to CPC powders. These HNTs were not loaded with DEX or any other growth factors. Mouse OBs were used for seeding on these scaffolds to evaluate the osteoconductive property of fabricated CPC. To evaluate the osteoinductive potential of our formulation with DEX-doped HNTs, four set of scaffolds were prepared (**Table 2**). Scaffolds in both groups were tested for cell viability, proliferation, ECM production, and alkaline phosphatase activity over a 14-day period. Standard histochemical staining techniques were used. We predicted that MSCs would differentiate into osteoblasts after the exposure to DEX-doped HNT/CPC composites.

2.6. Histochemical staining

As the CPC scaffolds were opaque, bright field microscopy or confocal microscopy images could not be taken. Accordingly, an indirect method of estimating the ECM deposition and amount was used. Collagen content was estimated using Picrosirius red (PS) staining and acidic mucopolysaccharides were estimated using Alcian blue (AB). To quantify staining, stained CP discs were destained measured for staining the dye concentration using UV-visible spectrophotometry. Indirect estimation was done using the destaining method. Glacial acetic acid 7% solution was used as destaining solution. After staining the hydrogel films, destaining solution was added to remove the dye that was fixed on the films. Destaining solution was then collected and measured for the concentration of staining the dye using UV spectrophotometry.

2.6.1. Picrosirius red staining

Picrosirius red is a specific collagen fiber stain and also is capable of detecting thin fibers. Media was removed from the wells and a wash was given with Dulbecco's phosphate buffered saline (DPBS) before fixing the cells using 95% ethanol. These fixed cells were stained with Picrosirius red for quantifying the amount of collagen secreted. The staining kit had three different solutions—A, B (Picrosirius stain), and C (hydrochloric acid—HCl). Solution A was added to the cells and removed after 5 min and solution B was added and was removed after an hour. A wash was given with solution C to remove excess staining. Glacial acetic acid 7% aqueous solution was used as de-staining solution. As the CPC scaffolds were too thick

Group	CPC composition
Group 1	CPC powder without HNTs
Group 2	CPC powder with 10% wt. HNTs
Group 3	CPC powder with 5% wt. DEX-doped HNTs and 5% wt. plain HNTs
Group 4	CPC powder with 10% wt. DEX-doped HNTs

Table 2. Control and experimental groups used in osteoinductive studies.

for light to penetrate, microscopic imaging and quantification were difficult to accomplish. To quantify staining, de-staining was used and measured for staining the dye concentration using UV-visible spectrophotometry.

2.6.2. Alcian blue staining

Alcian blue is used to stain sulfate glycosaminoglycans and proteoglycans in the extracellular matrix. The same procedure, as indicated above, was followed using Alcian blue solution as the dying reagent and destained samples were collected. These samples were later analyzed using a Thermo Scientific NanoDrop 2000c spectrophotometer.

2.6.3. Alkaline phosphatase (AP) assay

During *in vitro* bone formation, AP activity is greatly enhanced and hence used as a marker to evaluate the differentiation of MSCs towards osteoblastic lineage or maintenance of the osteoblast phenotype. It is easily detected using BCIP/NBT as a substrate, which stains cells blue-violet when AP is present. Alcohol fixed plates were washed with a buffer and carefully aspirated without disrupting the monolayer of cells. Enough BCIP/NBT substrate solution was added to just cover the monolayer and left in the dark for 5–10 min. It was then washed and destained using 7% glacial acetic acid for 5 min to quantify the AP activity. The solution was aspirated and analyzed using a NanoDrop 2000c spectrophotometer.

3. Results and discussion

3.1. SEM analysis

SEM was used to analyze the nature of the surface topography of CPCs. Surfaces in all formulations had granules of small and large size (**Figure 1**) No definitive difference could be observed visibility in these images between CPS with and without HNTS. Chitosan lactate was flakes or scales that were observed in thin layers around the particles of DCPA and TTCP (**Figures 1** and **2**). Granular particles of DCPA and TTCP are seen in a matrix of chitosan lactate. HNTs were also observed in few images distributed as clumps and as fine particles. As seen in **Figure 2**, aggregations of HNTs were observed distributed within the matrix of CPCs filling up the voids between the calcium and lactate particles. Cell viability and cell proliferation are largely dependent on the substrate surface, and cellular response to surface roughness is different depending on the cell type [32, 33]. Rough surfaces are preferred by many cell types for attachment and further functionality [33, 34]. Osteoblasts grown on surfaces with microtopography were stimulated towards differentiation as compared with a lack of specific bone marker expression when grown on smooth surfaces [35, 36]. SEM images of CPCs clearly indicate that all CPC formulations possess very rough surfaces and provide a conducive environment for cell attachment (**Figure 1**). This observation was confirmed by the cellular response of OBs and MSCs on the CPC surfaces.

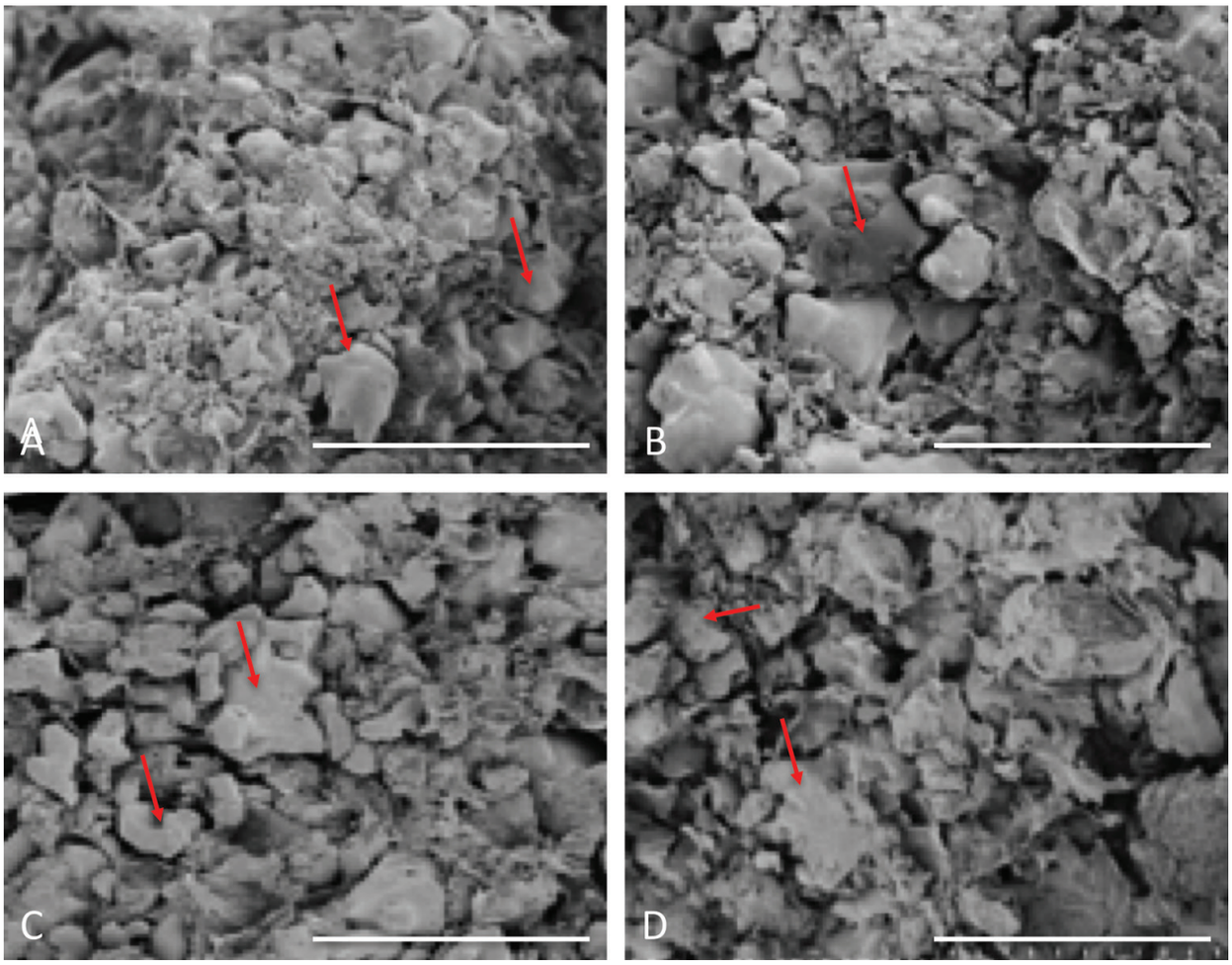

Figure 1. SEM images of CPCs with and without HNTs. (A) CPCs with 0% w/w HNTs (1200× magnification); (B) CPCs with 5% w/w HNTs (1200× magnification); (C) CPCs with 10% w/w HNTs (1500× magnification); and (D) CPCs with 15% w/w HNTs (1500× magnification). (A) and (B) scale bar = 40 microns; (C) and (D) scale bar = 30 microns. Red arrow = chitosan lactate.

3.2. Compression strength

Specimens made for the compression test were analyzed for maximum compressive strength and peak load taken before they were fractured. Of the various combinations of calcium salts and setting liquid salts tested, only those samples that had anti-washout property and good compressive strength were chosen. Most of the samples had decent compressive strength when dry, but upon placing them in an aqueous environment, they became soft and collapsed. Specimens made with TTCP and DCPA using chitosan as a setting liquid had good mechanical properties. As chitosan is soluble only in acidic solutions, aqueous solution of chitosan in acidic water was used. This resulted in elution of acid into SBF while testing for their anti-washout property. The pH of SBF was maintained at 7.40, but when these samples were immersed in SBF, the pH of the solution increased as high as pH 2.0. Hence, in-spite-of having good mechanical properties, these samples were not selected as it would create hostile microenvironment for cells. To prevent cytocompatibility issues, chitosan lactate was, accordingly, selected as the setting liquid as it was soluble in neutral water. When all samples were

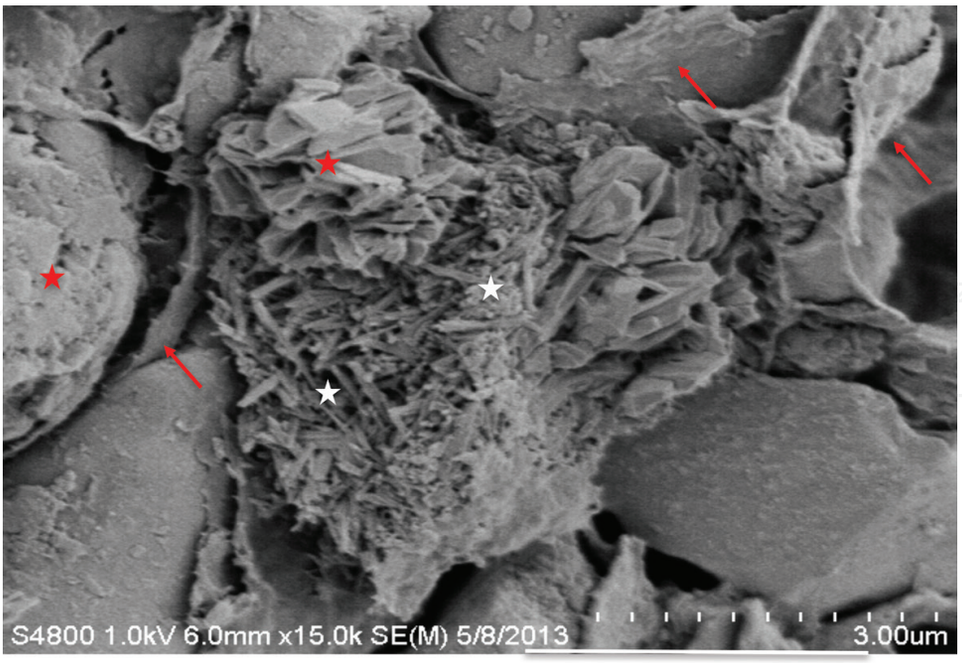

Figure 2. Scanning electron micrograph of CPC added with 5% wt. HNTs showing aggregation of HNTs. Red arrows = chitosan lactate flakes. Red star = calcium phosphate particles. White star = HNTs concentrations.

tested, the composition with the most desired properties was an equimolar mixture of TTCP and DCPA in the solid phase with chitosan lactate as the liquid phase.

Different concentrations of HNTs were added to this composition. These compositions were then tested for compression and flexural strengths. The addition of HNTs has an observable and significant change in the compressive strengths of CPCs (**Figure 3A**). Peak compressive strength was seen in groups that were added with 5% wt. HNTs. Peak compression pressure of 16.48 ± 0.95 MPa was observed for CPCs that were added with 5% wt. HNTs. CPCs that were not added with HNTs had a compressive strength of 11.65 ± 2.24 MPa. Compressive strength of CPCs is increased by 41.47% upon the addition of 5% of HNTs. At concentrations of 10 and 15% wt. HNTs, compressive strength of CPCs was recorded as 14.43 ± 1.64 MPa and 13.54 ± 1.67 MPa. Minimum of five samples in each group were tested and statistical analysis was performed on the data sets. One way ANOVA was done to analyze the statistical significance among the four groups. Results suggest that there is a significant difference in the means of all four groups at $\alpha = 0.05$. Post hoc analysis was done to identify the group with the highest mean compressive strength. Results from Tukey's HSD suggest that groups containing 5% wt. HNTs have the highest mean compressive strength.

Addition of nanoparticles in the matrix of CPCs improves the compression strength up to certain concentration and beyond this concentration no significant improvement was observed. The optimal concentration for this composition was observed to be at 5% wt. The particle size of TTCP contributes an important role in determining the compressive strength of CPCs. Smaller particles attribute for increased strength compared to larger particles. As shown in **Figure 3B**, at a particle size of 1.9 ± 0.31 μm, the compressive strength of CPCs was 23.49 ± 1.36 MPa. Larger particles with a diameter of 4.1 ± 1.15 μm had a peak compression strength of 8.25 ± 2.56 MPa. Particles with an average diameter of 2.4 ± 0.42 μm had a compression strength

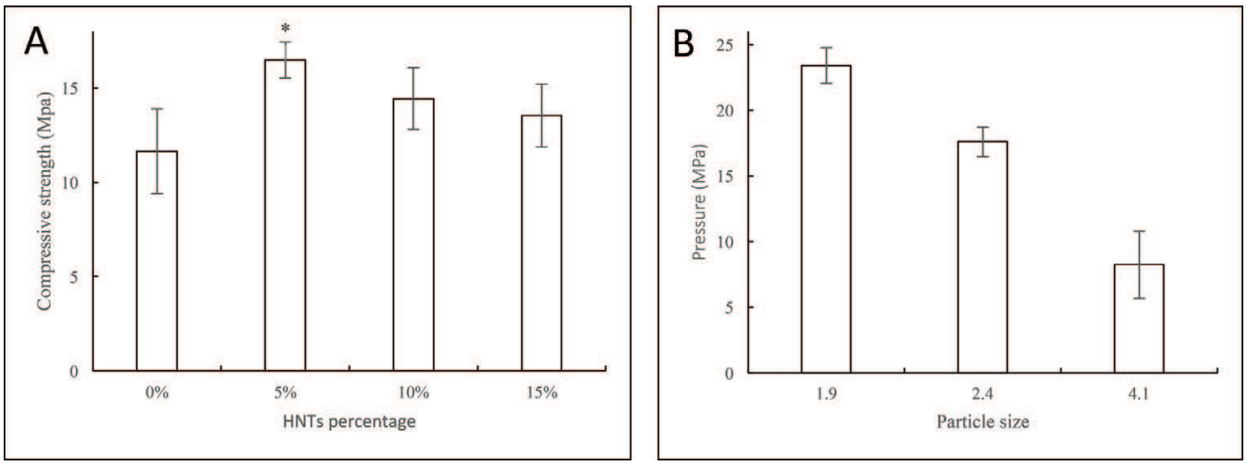

Figure 3. (A) Compressive strength of CPCs with varying amount of HNTs. (B) Compression strength as a function of particle size of TTCP. Error bars = standard deviation.

of 17.59 ± 1.13 MPa. It can be inferred that smaller particles may be arranged in a compact manner resulting in smaller voids between the particles and thus resulting in greater compression strengths of CPCs. This improvement in compression strength by the addition of HNTs can be useful in applications where primary forces acting on cements are compression. Bone cements used in vertebral augmentation are primarily subjected to compressive forces and the CPC/HNTs composite may be of use in this surgical procedure.

Much research was directed towards improvement of CPCs by introducing additives in solid and liquid phases. Improvements were observed in mechanical strengths, setting times, bioactivity, and degradability. Addition of gelatin and chitosan resulted in increased setting time, improved cell adhesion and ECM formation, and improved compressive strengths. Addition of other polymers including collagen, alginate, hyaluronate, cellulose, and synthetic polymers had various effects depending on the CPC composition and the amount of polymer [37, 38].

3.3. Flexural strength

Three-point bending test was performed to evaluate the flexural strength of CPCs (**Figure 4A**). Flexural strength of control group containing just DCPA, TTCP, and chitosan lactate was recorded as 13.86 ± 2.45 MPa. Addition of HNTs at 5% wt. improved the strength to 17.12 ± 2.49 MPa. This increase was not statistically significant at $\alpha = 0.05$. CPCs containing 10 and 15% wt. HNTs had flexural strengths of 15.38 ± 0.26 MPa and 17.41 ± 1.45 MPa, respectively. This trend of flexural strengths is graphically represented in **Figure 4B**. The standard deviation error bars in **Figures 3** and **4** may be attributed to air gaps formed while preparing the bone cement and loading them into the molds. Presence of air pockets can reduce the compression and flexural strength of cements. This may be avoided by using a vacuum chamber to mix and prepare the specimens.

The inability to provide significant resistance to applied mechanical loads has limited CPCs to non-load-bearing, mostly craniofacial applications [37–39]. Their toughness and fatigue resistance are much less than those of cortical bone. The incorporation of a polymer during the CPC liquid phase increases ductility, allowing for a higher deformation before breaking [39, 40]. Moreover, polymer fiber reinforcement has been extensively explored as a strategy to increase the toughness and strength of cements [41].

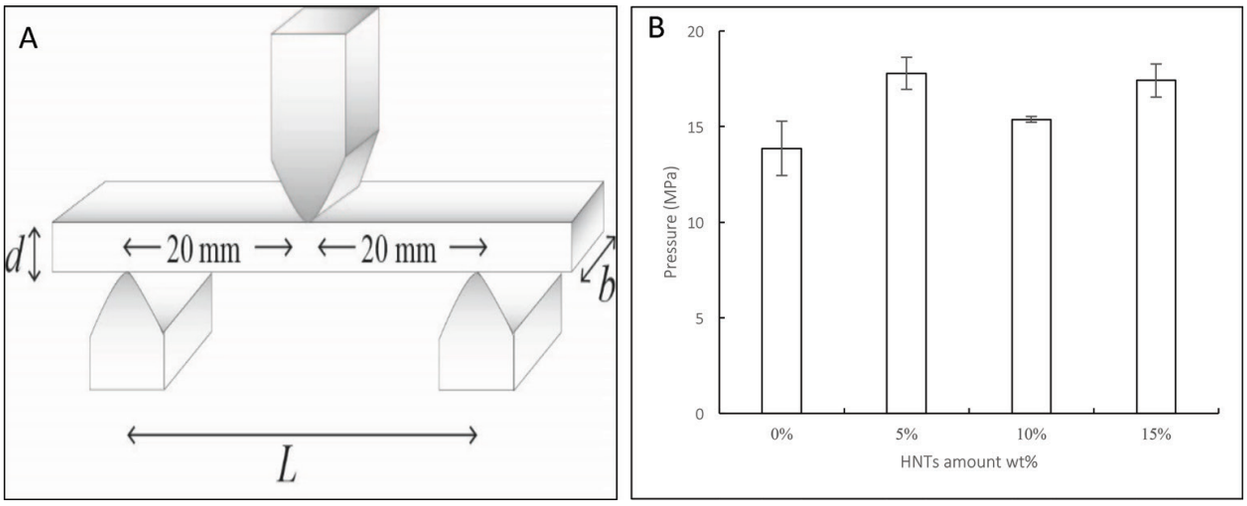

Figure 4. (A) Flexural test method. (B) Flexural strength of CPCs with varying amount of HNTs. Error bars = standard deviation.

One explanation for a portion of the gain in material strength could be HNT addition to the CPC cement. HNTs have been widely used as a nanofiller for the modification of nanocomposite materials [24, 25, 27]. HNTs have been used to increase surface area and impart high surface reactivity, improving mechanical and overall strength (see Zhang et al. for an excellent review [42]). To achieve the increase in mechanical strength, thermal stability, and toughness HNTs has been combined into a variety of polymers. Examples of polymer studied modification by HNTs include: poly(butylene succinate) [44], polyamide [12, 45], styrene-butadiene [46], epoxy [47], poly(methyl-methacrylate) [48], and chitosan [43]. In our case, we speculate that HNTs distribution the CPC cement fills voids resulting in the increase of mechanical strength by preventing crack propagation. HNTs have been suggested as mechanism nanoparticle deflect or absorb a propagating crack, thus preventing the formation of weak points and improving strengths. However, when the HNT concentration exceeds a certain value, the CPC deformability decreased sharply. This may be because of the pattern of HNT dispersion [47]. The interfacial binding between HNT/chitosan composites was proposed as resulting from hydrogen bonding and electrostatic interactions and a uniform dispersion results in a uniform interfacial-binding matrix and favorable to force conduction [43]. In contrast, too many HNTs and HNT clustering may inhibit the dispersion state and create interfacial gaps, which are easy to break.

3.4. FTIR analysis

The final setting product of apatite cements was hypothesized to be hydroxyapatite. To evaluate the end-product formation, FTIR analysis was used. A comparison of IR spectra of CPC control, CPCs (no HNTs added), CPCs with 5% HNTs, and hydroxyapatite is shown in **Figure 5**. Band of peaks seen at wavenumber 900–1200 cm^{-1} are due to PO + 4 groups present in all the test samples. Peaks at 1450 cm^{-1} are characteristic of the CO_3^{2-} group found in HA. Peaks at 3100–3700 cm^{-1} are due to the —OH groups of hydroxyapatite. Comparing peaks for the —OH group, we observe that CPCs with HNTs have stronger peak than control CPCs. This observation can be attributed to the presence of HNTs that acted as seeding/nucleating agents facilitating the precipitation of hydroxyapatite crystals.

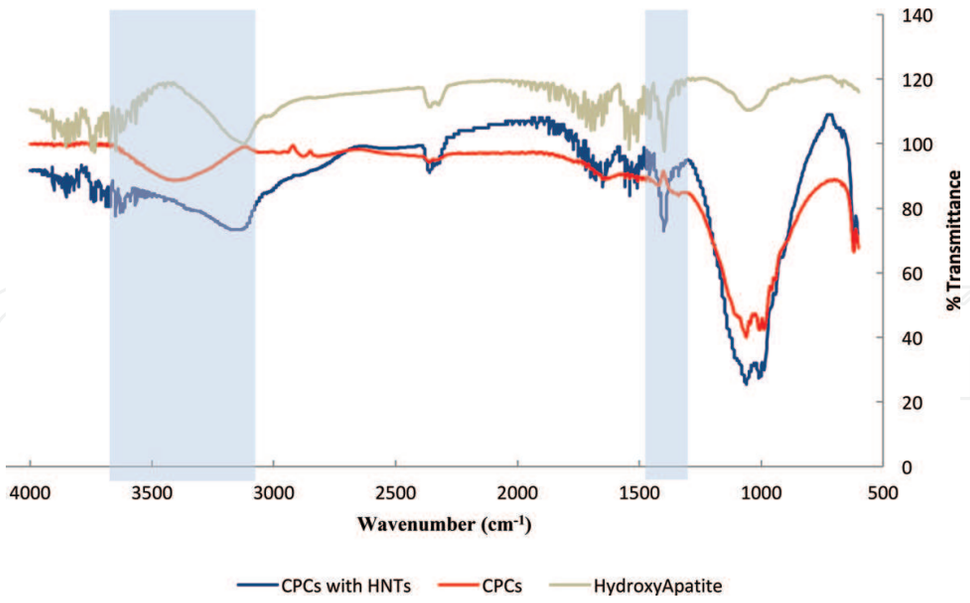

Figure 5. FTIR spectra of HA and CPCs with and with HNTs. Peaks at 1450 cm^{-1} and 3100–3700 cm^{-1} are characteristic of HA (CO_3^{2-} and —OH groups, respectively).

3.5. Dexamethasone elution profile

Drug elution was studied using 50 mg of DEX loaded HNTs (**Figure 6A**). It can be observed that there is an initial burst release from HNTs during the first 10 h of release and from then onwards it was sustained. This 50 mg elution form of HNTs is above the desired micro to nanomolar range to stimulate the differentiation of MSCs towards osteoblastic lineage. DEX release from scaffolds was also studied using scaffolds with only 5% of HNTs loaded with DEX. It can be observed that drug release was slow and the concentration of drug released from scaffolds is much lower compared to HNTs. **Figure 6B** shows the release of DEX from scaffolds. The drug release may be even more extended during scaffolds degradation exposing more HNTs to extracellular fluids (*in vivo*). Drug release from CPC scaffolds was less compared to HNTs. This may be attributed to the surface release and doped HNTs in the matrix did not have contributed to this release.

3.6. Cell proliferation

The viability of HOBs on the surface of the CPC scaffolds was analyzed at days 3, 7, and 14 (**Figure 7**). The absorbance values of the XTT assay reflects the mitochondrial activity of the live cells. The absorbance values across the 14-day period indicate that all samples showed no cytotoxic effects. The mean values of absorbance also varied strongly with the HNT concentration. On day 3, a 20.35% increase in absorbance values was observed for control CPC scaffolds when compared to wells containing only cells. On addition of 5% HNTs to the CPC scaffolds, 28.3% significant increase in the absorbance value was noticed. For 10 and 15% HNT absorbance was 9.8 and 12.8% larger, respectively. But, when compared with control CPC scaffold (no HNTs added), 8.7 and 6.1% decrease in the absorbance values for 10 and 15% CPC-HNT scaffolds were seen. By day 7, absorbance was larger for CPC scaffolds than for control wells. Wells containing 5% HNT samples showed 26.7% larger absorbance compared to CPC

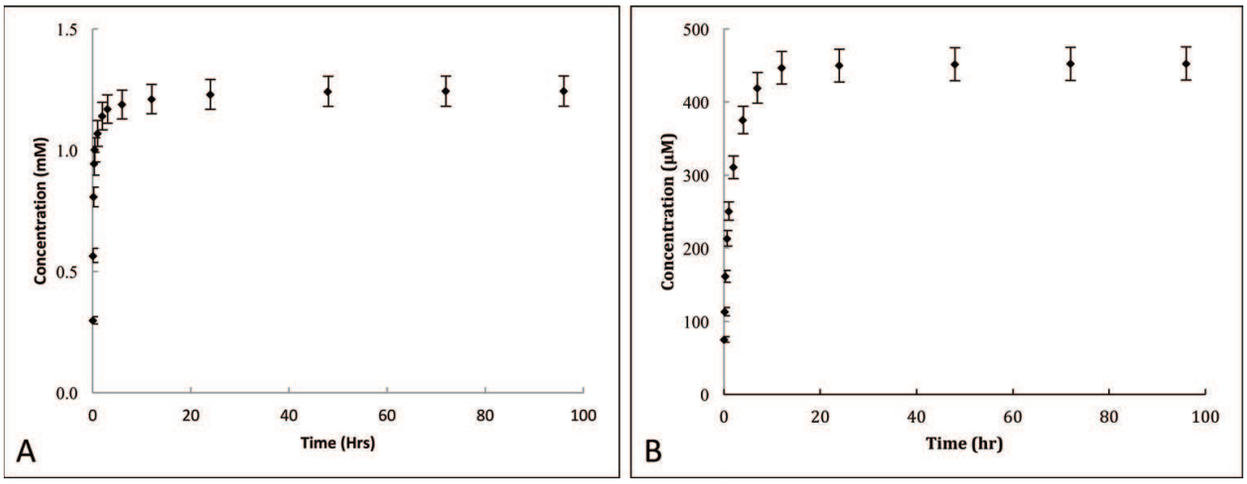

Figure 6. (A) Dexamethasone elution from loaded HNTs. (B) Dexamethasone release from CPC scaffolds loaded with DEX-doped HNTs.

samples without HNTs. CPCs with 10% HNTs had the highest absorbance value. Finally, at day 14, all wells containing CPC scaffolds showed higher absorbance values than control wells and it was the largest in scaffolds with 15% HNTs. The results further suggest that HNT/CPC composites are cytocompatible and enhance the osteoblast viability of the osteoblast cells. In addition, further increase in viability (cell growth) was seen with HNT addition.

3.7. Histochemical staining of HNT-doped CPC discs

As all CPC scaffolds were opaque, bright field microscopy or confocal microscopy micrographs were unable to be taken. An indirect method of estimating ECM production was

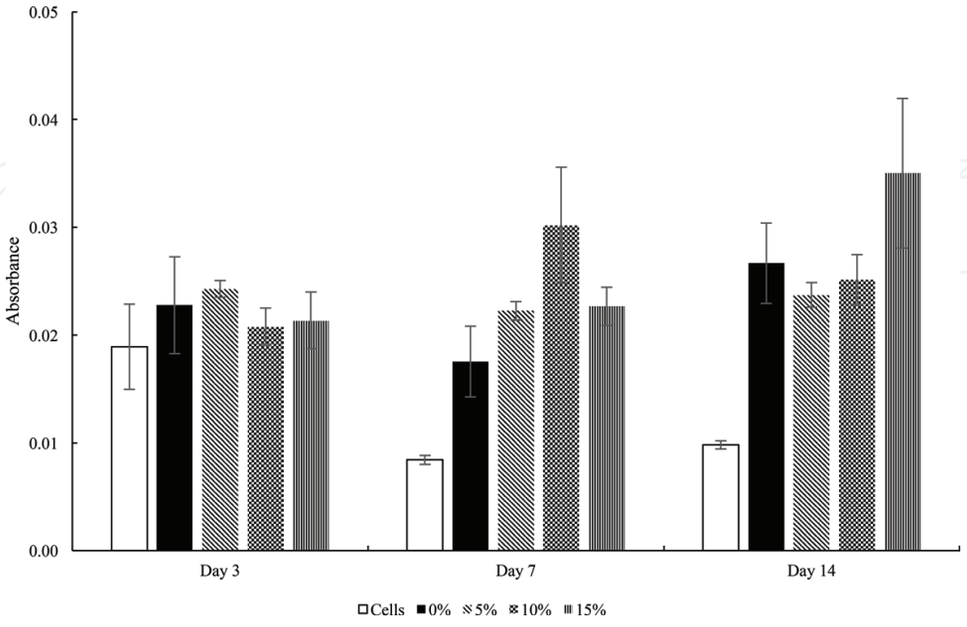

Figure 7. Cell viability assessed in human osteoblast culture on different CPC-HNT scaffolds (mean ± SD; n = 6).

employed using a staining and destaining method. Collagen content was estimated using the Picrosirius red stain, the presence of acidic mucopolysaccharides using an Alcian blue stain, and alkaline phosphatase activity was examined to confirm the osteoblastic phenotype of cells cultured of HNT/CPC discs.

3.7.1. Picrosirius red staining (PSR)

Graphical representation of PSR stain absorbance is shown in **Figure 8**. Higher absorbance indicates greater collagen content secreted by osteoblasts on the scaffolds. All test groups supported collagen production and throughout the length of the experimental period. On average, a higher amount of collagen synthesis was observed on day 14 stain as compared to day 7. However, there was no significant difference in the amount of collagen synthesized among all the groups on given day.

3.7.2. Alcian blue staining

Alcian blue staining was used to determine the acidic mucopolysaccharides synthesis. **Figure 9** is graphical representation of Alcian blue staining for all scaffolds over the testing period. Higher absorbance indicates higher acidic mucopolysaccharides synthesis. On day 7, acidic mucopolysaccharides synthesis was almost same across all CPC scaffold groups. Day 14 staining showed an improvement in mucopolysaccharide synthesis with an increase in the HNT concentration. CPC scaffolds with 15% HNTs showed the highest level of Alcian

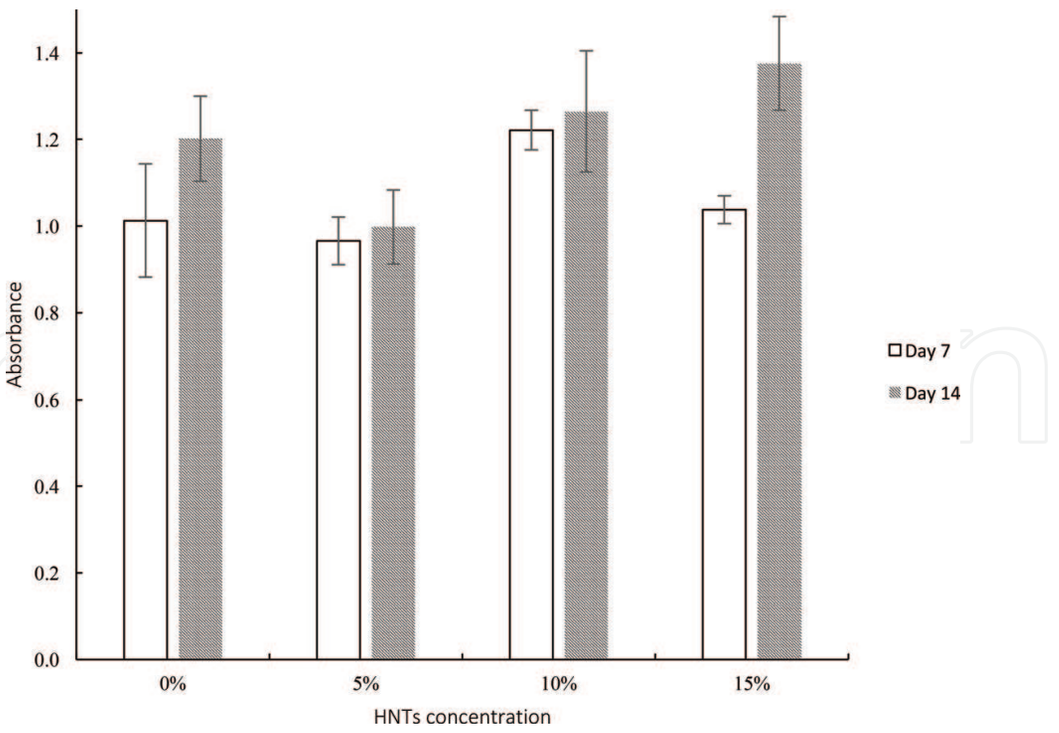

Figure 8. Destained well-plates showing red color, due to Picrosirius red, staining on and around osteoblast seeded CPC scaffolds indicating the presence of collagen. A = 7 days in culture and B = 14 days in culture. (C) Absorbance values for different HNT concentrations at day 7 and 14.

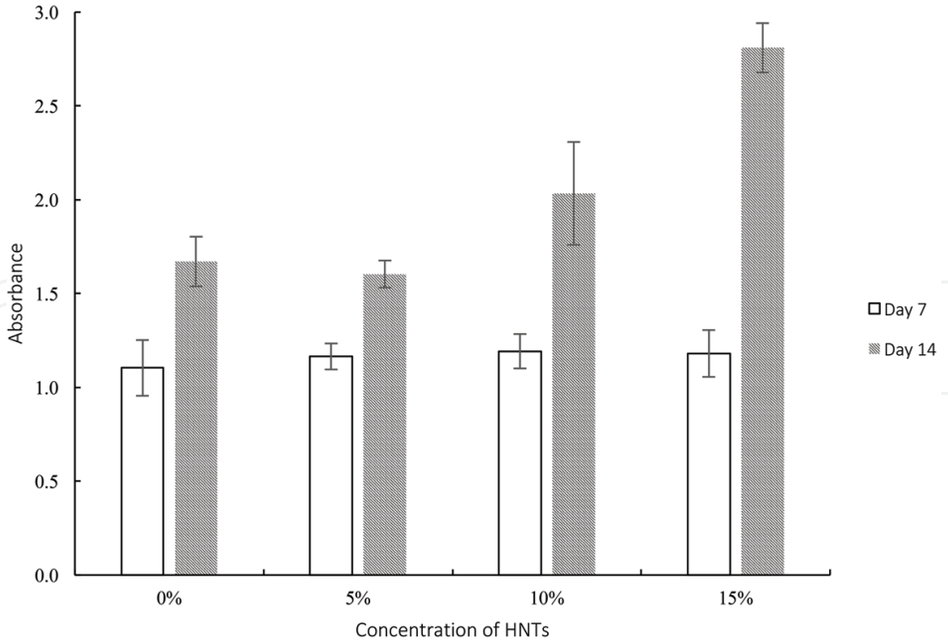

Figure 9. Destained well-plates showing blue color, due to Alcian blue dye, on and around CPC scaffolds indicating the presence of acid mucosubstances. A = 7 days in culture and B = 14 days in culture. (C) Absorbance values for different HNT concentrations at day 7 and day 14.

blue staining indicating the higher acidic mucopolysaccharides synthesis. However, there was no significant difference in the amount of collagen synthesized among all the groups on given day.

The Picrosirius red and Alcian blue staining results suggest that CPC surfaces are conducive for osteogenesis and cell viability. Production of ECM molecules is a critical factor during bone tissue regeneration.

3.7.3. Alkaline phosphatase activity (ALP)

Preservation of the osteoblastic phenotype in OB cells was assayed using ALPase activity. It was observed that all CPC groups had a strong ALPase activity showing the preservation of the osteoblast phenotype (**Figure 10**). From the graph, it can be inferred that the cells had enhanced ALPase activity on day 14 compared to day 7. A pronounced increase in ALPase activity was seen in CPC discs without HNTs and CPCs with 10% wt. HNTs. There was, however, no statistical difference among groups on a given day of assay. All histochemical staining results suggest that CPC surfaces are conducive for osteoblast attachment, proliferation, and synthesis of an organic matrix that was subsequently mineralized. Osteogenesis and cell viability are the critical requirements for bone tissue regeneration.

3.8. Histochemical staining of DEX-doped HNT/CPC discs

As with the HNT/CPC discs, an indirect method of estimating ECM production was employed using the same staining methods and destaining protocols.

http://dx.doi.org/10.5772/intechopen.74341

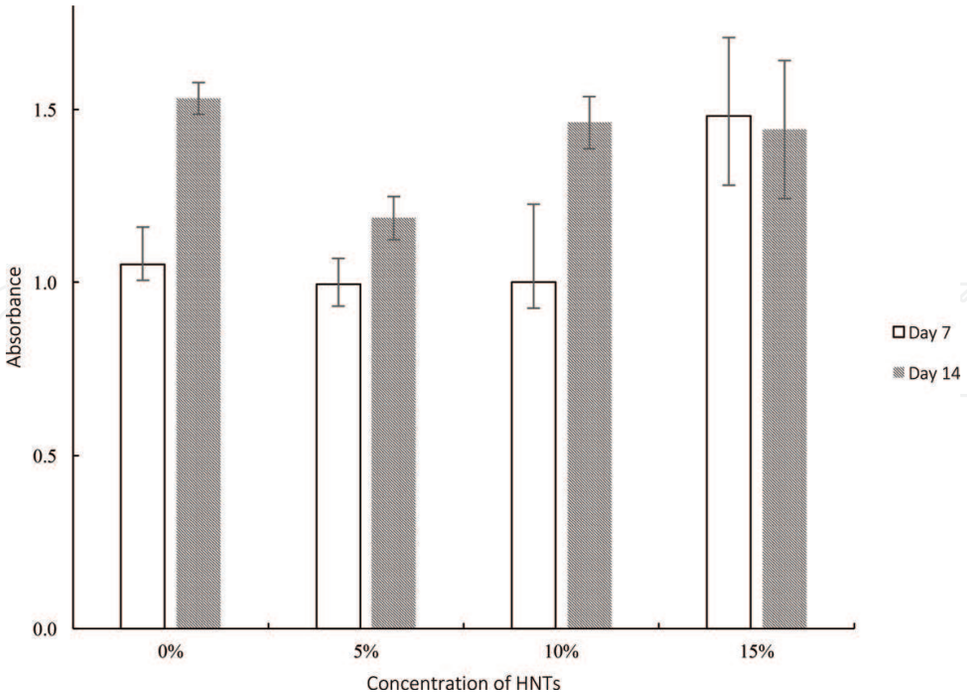

Figure 10. Comparison of absorbance values for samples collected at different concentrations of HNTs at day 7 and day 14 for ALPase activity.

3.8.1. Picrosirius red staining (PSR)

MSC collagen production was observed across all the test groups and throughout the length of the experimental period (**Figure 11**). Collagen synthesis remained almost same for any given group on all the days except for Group 3. By day 7 and 14, these scaffolds were stained equally compared to the rest other scaffold groups. By the end of day 14, all the scaffolds were equally stained with PSR stain referring to similar amount of collagen production by cells on all the scaffolds. However, no significant difference in the amount of collagen is synthesized among all the groups on given day. In comparing OB and MSC collagen synthesis on CPC/HNT discs, the pattern observed was similar for Group 1 (CPCs no HNTs) and OB Group #3/MSC Group #2 (CPCs with 10% HNTs).

3.8.2. Alcian blue staining

Each group of scaffolds followed a different trend for each day of experiment in terms of acidic mucopolysaccharide synthesis (**Figure 12**). Group 1 scaffolds had an increase in staining for day 3 and slight decrease on the following days 7 and 14. Staining on Group 2 scaffolds had deep staining on day 7, while on rest other days, similar amount of staining was observed. Group 3 scaffolds showed a similar staining for all the test days, in contrast, Group 4 scaffolds were deeply stained on day 14 compared to other days (**Figure 12**). Results from Picrosirius red and Alcian blue stains suggest cytocompatibility of these scaffolds with bone marrow stromal cells. The presence of dexamethasone does not appear to enhance or decrease the ECM synthesis as revealed by histochemical staining.

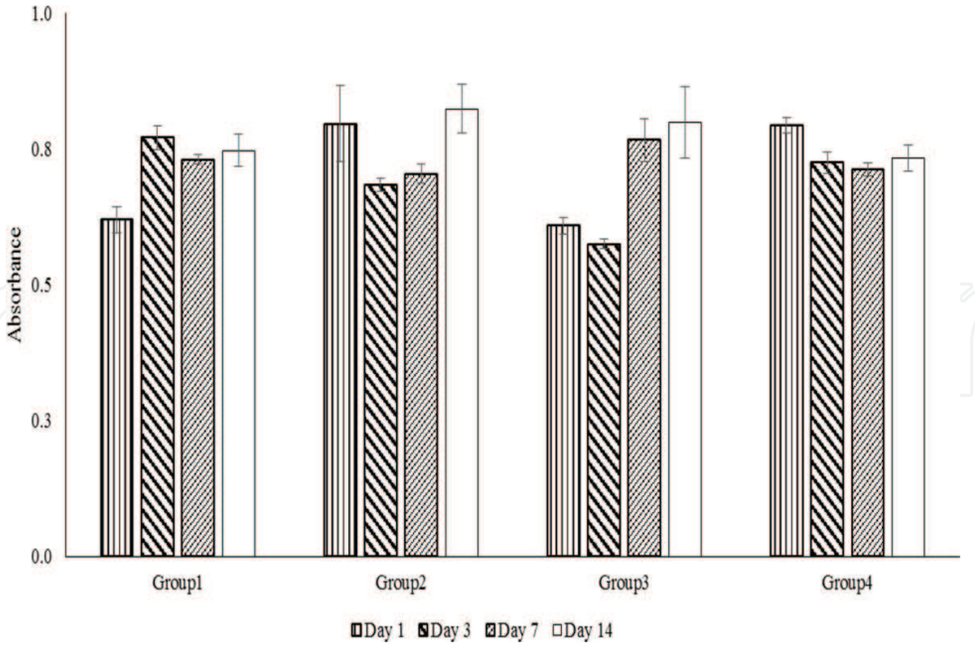

Figure 11. Picrosirius red staining. Collagen synthesis was consistent and steady across all study groups.

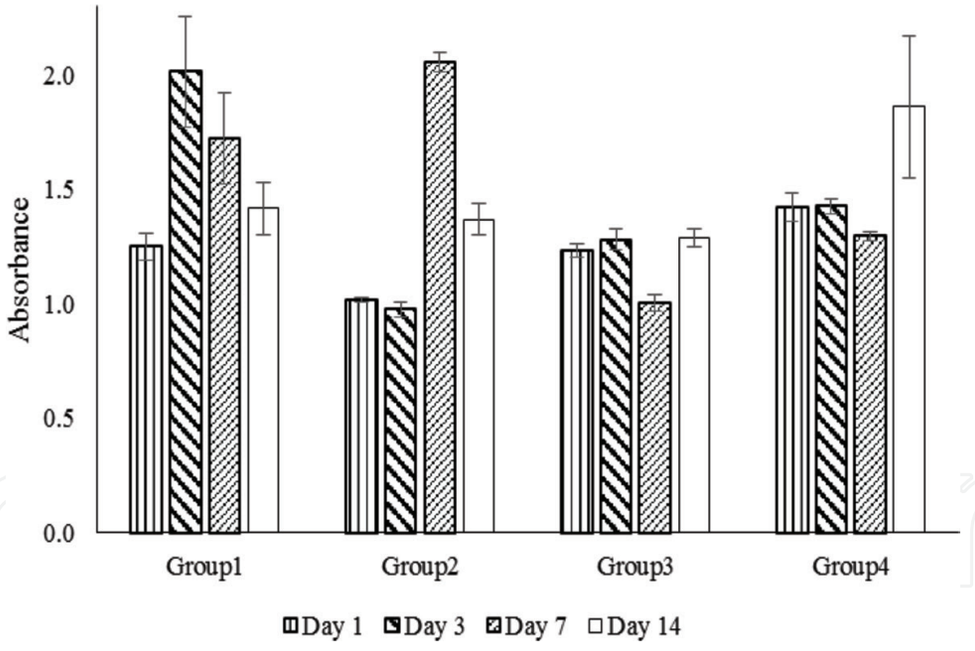

Figure 12. Alcian blue staining for osteoinductive scaffolds. A different trend was observed in terms of acidic mucopolysaccharide synthesis for all four groups.

3.8.3. Alkaline phosphatase activity

According to the hypothesis, scaffold Groups 3 and 4 would induce differentiation of BSCs towards osteoblastic lineage as they contained different concentrations of DEX- doped HNTs. Hence, more alkaline phosphatase activity was predicted in these groups. Staining results of

http://dx.doi.org/10.5772/intechopen.74341

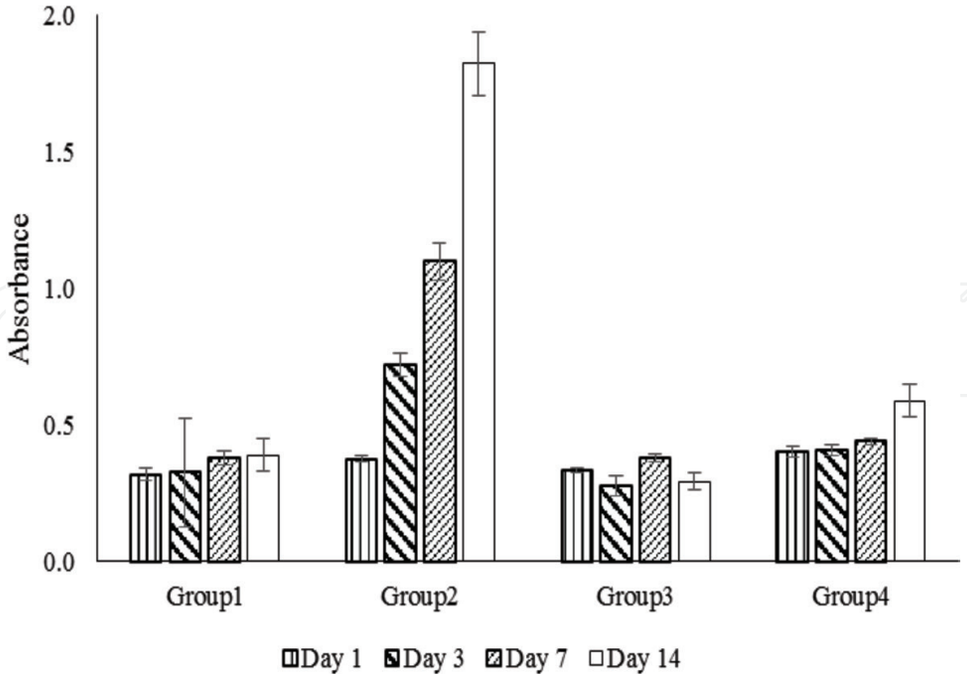

Figure 13. Alkaline phosphatase activity assay for osteoinductive scaffolds.

alkaline phosphatase assay are shown in **Figure 13**. Differentiation was more pronounced on Group 2 scaffolds that contained empty HNTs. Scaffolds of Groups 3 and 4, containing DEX loaded HNTs did not induce osteoblastic differentiation in the BSCs. Cell culture wells containing Group 2 scaffolds were deeply stained in purple while the rest other wells were stained slightly or none. Group 2 scaffolds' alkaline phosphatase activity was significantly higher on day 14 compared to other groups. Inability of Group 3 and 4 scaffolds to induce differentiation may be attributed to very high concentrations of DEX released. The optimum concentration of DEX needed to induce the osteogenic differentiation is 10–7 [49–51]. In the CPC discs doped with DEX, DEX may have been eluted in excess and thus had an inhibitory effect.

The ability of HNTs alone (no DEX) to induce osteogenic differentiation was previously reported using montmorillonite-doped biopolymers [52]. It may be inferred from this study and the study by Ambre et al. that many aluminosilicate clays may be inherently osteoinductive [53].

4. Conclusions and future work

We conclude that CPCs fabricated using TTCP and DCPA as the solid phase and 10% chitosan lactate solution as the setting liquid and doped with HNTs have an osteoconductive nature as evidenced by a production of an abundant ECM synthesis and alkaline phosphatase activity. Surface roughness was increased with HNT addition which favors cell attachment, proliferation, and ECM synthesis. Halloysite increased the compressive strength of CPCs. The composition of CPCs after setting was analyzed using FTIR which reveals that the addition of HNTs increased HA production by acting as seeding agents for the precipitation of

HA. CPC with DEX-doped HNTs showed an extended release of DEX from CPC scaffolds. DEX-loaded HNTs were used in varying concentrations in the fabrication of osteoinductive scaffolds. Osteoinductive scaffolds were seeded with MSCs to evaluate their osteoinductive nature. Our results suggest that HNTs with DEX loaded in the scaffolds started inducing differentiation in MSCs after 14 days while scaffolds with empty HNTs started inducing differentiation towards osteoblastic lineage after 3 days. At the end of 14th day, scaffolds containing non-loaded HNTs had the highest amount of alkaline phosphatase activity suggesting maximum differentiation of BSCs to osteoblastic phenotype. HNTs promoting differentiation of BSCs to osteoblastic phenotype can be explored further using different compositions. HNTs loaded with different drugs, antibiotics, growth factors, and chemotherapeutic agents can be used in fabricating CPCs. Addition of other polymers can also be considered to enhance the CPC mechanical properties further. *In vivo* experiments are being conducted in small animals to evaluate the tissue formation properties effectiveness of the CPCs fabricated.

Acknowledgements

The authors would like to acknowledge the Louisiana's Governor's Biotechnology Initiative, LASPACE and the Louisiana Board of Regents OPT-IN program for their funding support (awarded to Dr. David K. Mills).

Conflicts of interest

The authors declare that they have no conflicts of interest.

Author details

Udayabhanu Jammalamadaka[1], Karthik Tappa[1] and David K. Mills[2]*

*Address all correspondence to: dkmills@latech.edu

1 Center for Biomedical Engineering and Rehabilitation Science, Louisiana Tech University, Ruston, LA, USA

2 Center for Biomedical Engineering and Rehabilitation Science and the School of Biological Sciences, Louisiana Tech University, Ruston, LA, USA

References

[1] DiMaio FR. The science of bone cement: A historical review. Orthopedics. 2002;**25**(12): 1399-1407

[2] Webb JCJ, Spencer RF. The role of polymethylmethacrylate bone cement in modern orthopaedic surgery. Journal of Bone and Joint Surgery. British Volume (London). 2007;**89**(7):851-857

[3] Lidgren L, Robertson O. Acrylic bone cements: Clinical developments and current status. Scandinavia. The Orthopedic Clinics of North America. 2005;**36**(1):55-61

[4] Kühn K-D. Properties of bone cement: What is bone cement. In: Breusch S, Malchau H, editors. The Well-Cemented Total Hip Arthroplasty. Heidelberg: Springer Medizin Verlag; 2005. pp. 52-59

[5] Gough JE, Downes S. Osteoblast cell death on methacrylate polymers involves apoptosis. Journal of Biomedical Materials Research. 2001;**57**(4):497-505

[6] Stańczyk M, van Rietbergen B. Thermal analysis of bone cement polymerization at the cement-bone interface. Journal of Biomechanics. 2004;**37**(12):803-810

[7] Lautenschlager EP, Jacobs JJ, Marshall GW, Meyer PR. Mechanical properties of bone cements containing large doses of antibiotic powders. Journal of Biomedical Materials Research. 1976;**10**(6):929-938

[8] Vaishya R, Chauhan M, Vaish A. Bone cement. Journal of Clinical Orthopaedics and Trauma. 2013;**4**(4):157-163. http://doi.org/10.1016/j.jcot.2013.11.005

[9] Bistolfi A, Massazza B, Verné E, Massè E, Deledda DA, Ferraris S, Miola M, Galetto F, Crova M. Antibiotic-loaded cement in orthopedic surgery: A review. ISRN Orthopedics. 2011:1-8

[10] Brown WE, Chow LC. A new calcium phosphate setting cement. Journal of Dental Research. 1983;**62**:672-678

[11] Friedman CD, Costantino PD, Takagi S, et al. BoneSource hydroxyapatite cement: A novel biomaterial for craniofacial skeletal tissue engineering and reconstruction. Journal of Biomedical Materials Research Part B: Applied Biomaterials. 1998;**43**:428-432

[12] Komlev VS, Fadeeva IV, Gurin N, Shvorneva LI, Bakunova NV, Barinov SM. New calcium phosphate cements based on tricalcium phosphate. Doklady Chemistry. Apr. 2011;**437**(1):75-78

[13] Lee KY, Park M, Kim HM, Lim YJ, Chun HJ, Kim H, et al. Ceramic bioactivity: Progresses, challenges and perspectives. Biomedical Materials. 2006;**1**:R31-R37

[14] Dorozhkin SV, Epple M. Biological and medical significance of calcium phosphates. Angewandte Chemie, International Edition. 2002;**41**:3130-3146

[15] Kühn K-D. Properties of bone cement. In: Breusch S, editor. The Well-Cemented Total Hip Arthroplasty. Heidelberg: Springer MedizinVerlag; 2005. pp. 52-59

[16] Ducheyne P, Qiu Q. Bioactive ceramics: The effect of surface reactivity on bone formation and bone cell function. Biomaterials. 1999;**20**:2287-2303

[17] Radin S, Reilly G, Bhargave G, et al. Osteogenic effects of bioactive glass on bone marrow stromal cells. Journal of Biomedical Materials Research. Part A. 2005;**73**:21-29

[18] Albrektsson T, Johansson C. Osteoinduction, osteoconduction and osseointegration. European Spine Journal. 2001;**10**:S96-S101

[19] Barinov SM, Komlev VS. Calcium phosphate bone cements. Inorganic Materials. 2011; **47**(13):1470-1485

[20] Bohner M. Reactivity of calcium phosphate cements. Journal of Materials Chemistry. 2007;**17**(38):3980-3992

[21] Ginebra MP. Cements as bone repair materials. In: Planell JA, editor. Bone Repair Biomaterials. Cambridge, England: Woodhead Publishing Limited; 2009. pp. 271-308

[22] Shchukin DG, Sukhorukov GB, Price RR, Lvov YM. (2005) Halloysite nanotubes as biomimetic Nanoreactors. Small. 2005;**1**:510-513

[23] Abdullayev E, Lvov Y. Halloysite clay nanotubes for controlled release of protective agents. Journal of Nanoscience and Nanotechnology. 2011;**11**(11):10007-10026

[24] Du M, Guo B, Jia D. Newly emerging applications of halloysite nanotubes: A review. Polymer International. 2010;**59**(5):574-582

[25] Liu M, Wu C, Jiao Y, Xiong S, Zhou C. Chitosan/halloysite nanotubes bionanocomposites: Structure, mechanical properties and biocompatibility. International Journal of Biological Macromolecules. 2012;**5**:566-575

[26] Karnik S, Jammalaka U, Tappa K, Mills DK. Performance evaluation of nanoclay enriched anti-microbial hydrogels for biomedical applications. Heliyon. 2016;**2**(2):1-21

[27] Lee J-W, Park S-J, Kin TH. Improvement of interfacial adhesion of incorporated halloysite-nanotubes in fiber-reinforced epoxy-based composites. Applied Sciences. 2017;**7**:441. DOI: 10.3390/app7050441

[28] Lai X, Agarwal M, Lvov YM, Pachpande C, Varahramyan K, Witzmann FA. Proteomic profiling of halloysite clay nanotube exposure in intestinal cell coculture. Journal of Applied Toxicology. 2013;**33**:1316-1329

[29] Lovo Y, Aerov A, Fakhrulli R. Clay nanotube encapsulation for functional biocomposites. Advances in Colloid and Interface Science. 2014;**207**:189-198

[30] Bellani L, Giorgetti G, Riela S, Lazzara G, Scialabba A, Massaro M. Ecotoxicity of halloysite nanotube–supported palladium nanoparticles in Raphanus sativus L. Environmental Toxicology and Chemistry. 2016;**35**:2503-2510

[31] Wei W, Abdllayev E, Goeders A, Hollister A, Lvov L, Mills DK. Clay nanotube/poly(methyl methacrylate) bone cement composite with sustained antibiotic release. Macromolecular Materials and Engineering. 2012;**297**:645-653

[32] Khalili AA, Ahmad MR. A review of cell adhesion studies for biomedical and biological applications. International Journal of Molecular Sciences. 2015;**16**:18149-18184

[33] Chang H-I, Wang Y. Cell responses to surface and architecture of tissue engineering scaffolds, regenerative medicine and tissue engineering. In: Eberli D, editor. ISBN: 978-953-307-663-8Cells and Biomaterials. InTech; 2011

[34] Zan X, Sitasuwan P, Feng S, Wang Q. Effect of roughness on in situ biomineralized CaP-collagen coating on the osteogenesis of mesenchymal stem cells. Langmuir. 2016;**32**(7):1808-1817

[35] Hatano K, Inoue H, Kojo T, Tsujisawa T, Uchiyama C, Uchida Y. Effect of surface roughness on proliferation and alkaline phosphatase expression of rat calvarial cells cultured on polystyrene. Bone. 1999;**25**:439-445

[36] Lim JY, Hansen JC, Siedlecki CA, Runt J, Donahue HJ. Human foetal osteoblastic cell response to polymer-demixed nanotopographic interfaces. Journal of The Royal Society Interface. 2005;**2**:97-108

[37] Eliaz N, Noah Metoki N. Calcium phosphate bioceramics: A review of their history, structure, properties, coating technologies and biomedical applications. Materials. 2017;**10**(4):334. DOI: 10.3390/ma10040334

[38] Perez RA, Kim HW, Ginebra MP. Polymeric additives to enhance the functional properties of calcium phosphate cements. Journal of Tissue Engineering. 2012;**3**(1):1-20. DOI: 10.1177/2041731412439555

[39] Zhang JT, Tancret F, Bouler JM. Fabrication and mechanical properties of calcium phosphate cements (CPC) for bone substitution. Materials Science and Engineering: C. 2011;**31**(4):740-747. DOI: 10.1016/j.msec.2010.10.014

[40] Khashaba M, Moussa MM, Mettenburg DJ, Rueggeberg FA, Chutkan NB, Borke JL. Polymeric-calcium phosphate cement composites-material properties: In vitro and in vivo investigations. International Journal of Biomaterials. 2010;**2010**:223-239

[41] Ambard AJ, Mueninghoff L. Calcium phosphate cement: Review of mechanical and biological properties. Journal of Prosthodontics. 2006;**15**:321-328

[42] Zhang Y, Tang A, Yang H, Ouyang J. Applications and interfaces of halloysite nanocomposites. Applied Clay Science. 2016;**119**(1):8-17

[43] Liu M, Zhang Y, Wu C, Xiong S, Zhou C. Chitosan/halloysite nanotubes bionanocomposites: Structure, mechanical properties and biocompatibility. International Journal of Biological Macromolecules. 2012;**51**:566-575

[44] Wu W, Cao X, Luo J, He G, Zhang Y. Morphology, thermal, and mechanical properties of poly(butylene succinate) reinforced with halloysite nanotube. Polymer Composites. 2014;**35**:847-855

[45] Lecouvet B, Gutierrez J, Sclavons M, Bailly C. Structure property relationships in polyamide 12/halloysite nanotube nanocomposites. Polymer Degradation and Stability. 2011;**96**:226-235

[46] Guo B, Chen F, Lei Y, Liu X, Wan J, Jia D. Styrene-butadiene rubber/ halloysite nanotubes nanocomposites modified by sorbic acid. Applied Surface Science. 2009;**255**:7329-7336

[47] Deng S, Zhang J, Ye L. Halloysite–epoxy nanocomposites with improved particle dispersion through ball mill homogenization and chemical treatment. Composites Science and Technology. 2009;**69**:2497-2505

[48] Wei W, Abdllayev E, Goeders A, Hollister A, Lvov Y, Mills DK. Clay nanotube/ poly(methyl methacrylate) bone cement composite with sustained antibiotic release. Macromolecular Materials and Engineering. 2012;**297**:645-653

[49] Langenbach F, Handschel J. Effects of dexamethasone, ascorbic acid and β-glycerophosphate on the osteogenic differentiation of stem cells in vitro. Stem Cell Research & Therapy. 2013;**4**(5):117. http://doi.org/10.1186/scrt328

[50] Yuasa M, Yamada T, Taniyama T, Masaoka T, Xuetao W, Yoshii T, Sotome S. Dexamethasone enhances osteogenic differentiation of bone marrow- and muscle-derived stromal cells and augments ectopic bone formation induced by bone morphogenetic protein-2. PLoS One. 2015;**10**(2):e0116462 http://doi.org/10.1371/journal.pone.0116462

[51] Rimando MG, Wu H-H, Liu Y-A, Lee C-H, Kuo S-W, Lo Y-P, Tseng K-F, Liu Y-S, Lee OK. Glucocorticoid receptor and histone deacetylase 6 mediate the differential effect of dexamethasone during osteogenesis of mesenchymal stromal cells (MSCs). Science Reports. 2016;**30**(6):37371. DOI: 10.1038/srep37371

[52] Ambre AH, Katti DR, Katti KS. Nanoclays mediate stem cell differentiation and mineralized ECM formation on biopolymer scaffolds. Journal of Biomedical Materials Research. Part A. 2013;**101**(9):2644-2660

[53] Ambre AH, Katti DR, Katti KS. Biomineralized hydroxyapatite nanoclay composite scaffolds with polycaprolactone for stem cell-based bone tissue engineering. Journal of Biomedical Materials Research. Part A. 2015 Jun;**103**(6):2077-2101. DOI: 10.1002/ jbm.a.35342